Constrained port-Hamiltonian modeling and structure-preserving discretization of the Rayleigh beam ⋆

Cristobal Ponce [*,**], **Hector Ramirez** [**], **Yann Le Gorrec** [*], **Yongxin Wu** [*]

[*] *Université Marie et Louis Pasteur, SUPMICROTECH, CNRS, institut FEMTO-ST, F-25000 Besançon, France. Emails: {cristobal.ponce, legorrec, yongxin.wu}@femto-st.fr*

[**] *Departamento de Electrónica, Universidad Técnica Federico Santa María, Valparaíso, Chile. Emails: {cristobal.ponces, hector.ramireze}@usm.cl*

Abstract: This paper addresses the port-Hamiltonian modeling of the Rayleigh beam, which bridges the gap between the Euler-Bernoulli and Timoshenko beam theories. This balance makes the Rayleigh model particularly suitable for scenarios where Euler-Bernoulli assumptions are insufficient, but Timoshenko's complexity is unnecessary, such as in cases of moderate oscillations. The originality of the approach lies in deriving the Rayleigh beam model from the displacement field of the Timoshenko beam and incorporating an algebraic constraint consistent with Rayleigh beam theory. The resulting model is formulated as an infinite-dimensional port-Hamiltonian differential-algebraic equation (PH-DAE). A structure-preserving spatial discretization strategy is developed using the mixed finite element method, ensuring the preservation of the PH-DAE structure in the finite-dimensional setting. Numerical simulations demonstrate the accuracy and effectiveness of the proposed model and discretization approach.

Keywords: Port-Hamiltonian Systems; Differential-Algebraic Equations; Modeling; Rayleigh beam; Structure-preserving discretization.

1. INTRODUCTION

The port-Hamiltonian (PH) framework offers a modular approach to modeling physical systems while preserving energy and passivity, making it well-suited for passivity-based control and Lyapunov-based stability analysis (Duindam et al., 2009). Its structure effectively separates interconnection laws from constitutive relations and accommodates differential-algebraic equation (DAE) representations, which efficiently manage constraints (van der Schaft, 2000; Mehrmann and Unger, 2023).

Beam theories are fundamental for modeling slender structures in engineering, with applications in structural mechanics, robotics, and aerospace. The Euler-Bernoulli, Rayleigh and Timoshenko models provide varying levels of accuracy in beam dynamics. The Rayleigh model builds upon the Euler-Bernoulli theory by incorporating rotational inertia, making it suitable for moderate oscillations where Euler-Bernoulli assumptions are insufficient but Timoshenko's complexity is unnecessary. On the other hand, the Timoshenko model accounts for shear deformation and rotational inertia, offering a more precise description for thick beams or high-frequency vibrations (Labuschagne et al., 2009; Nguyen, 2017). In addition, reliable simulations and control design favor models that exhibit energy and passivity, such as PH representations, which are available for both Timoshenko and Euler-Bernoulli beams (Macchelli and Melchiorri, 2004; Cardoso-Ribeiro et al., 2016; Warsewa et al., 2021).

In terms of kinematics, the Timoshenko beam employs $n = 2$ generalized displacements and $m = 2$ generalized strains, leading to a first-order differential operator of size $m \times n = 2 \times 2$. The Euler-Bernoulli beam simplifies to $n = 1$ displacement and $m = 1$ strain due to its assumptions, resulting in a second-order operator of size $m \times n = 1 \times 1$. For the Rayleigh beam, a PH model has been proposed in (Ponce et al., 2023, Appendix D.8), where the kinematic relation involves a second-order operator of size $m \times n = 1 \times 2$. However, the direct application of this model complicates spatial discretization, particularly in ensuring stability and physical validity during finite element implementation. Mixed finite element methods (FEM) are effective for discretizing PHS by simultaneously treating energy and co-energy variables while preserving structure (Golo et al., 2004; Thoma and Kotyczka, 2022; Kinon et al., 2024). However, applying mixed FEM to the Rayleigh beam presents challenges; the stability and physical validity of approximate solutions require that the strain field dimension m be at least equal to the displacement field dimension n (Zienkiewicz et al., 2005, Chapter 10.4.3), a condition not satisfied by the Rayleigh

⋆ The authors acknowledge financial support from: Chilean ANID projects Becas/ Doctorado Nacional/ 2021-21211290, ECOS 220040, FONDECYT 1231896, BASAL AFB240002; the French ISITE-BFC project - CPHS2D - ANR-15-IDEX-0003, EIPHI Graduate School ANR-17-EURE-0002, IMPACTS Project ANR-21-CE48-0018; and the European MSCA Project MODCONFLEX 101073558.

model in (Ponce et al., 2023, Appendix D.8). Moreover, first-order operators are preferred for FEM discretization to mitigate numerical issues, such as spurious oscillations, poor convergence, and high computational costs (Christie et al., 1976; Suri, 1990; Engel et al., 2002).

To address these challenges, we propose a novel approach to derive the Rayleigh beam model based on the Timoshenko beam's kinematic assumptions and introducing an algebraic constraint consistent with Rayleigh beam theory. The resulting model is a PH-DAE system that captures the kinematics and energy assumptions of the Rayleigh beam while being described by a first-order differential operator. This approach also satisfies the dimensionality requirements essential for the stability and physical validity of approximate solutions obtained using mixed FEM. Our contributions are twofold. First, we derive an infinite-dimensional PH-DAE model for the Rayleigh beam using the extended Hamilton's principle (Bedford, 1985), leveraging the structural advantages of the PH framework while overcoming the limitations of traditional Rayleigh formulations. Second, we extend the Hellinger-Reissner (H-R) principle-based approach proposed in (Thoma and Kotyczka, 2022) for the structure-preserving mixed FEM discretization of the PH-DAE, integrating the constraint directly within the FEM framework. This ensures that the finite-dimensional model retains the PH-DAE structure and defines appropriate boundary conditions (BCs).

The paper is structured as follows: Section 2 provides background on PH beam models. Section 3 discusses the modeling of the Rayleigh beam as a PH-DAE system and its structure-preserving spatial discretization. Section 4 presents simulations to validate the proposed approach. Finally, Section 5 concludes and discusses future work.

2. PRELIMINARIES

In this section we provide an overview of the fundamental physical principles that will be employed in later sections, along with definitions related to infinite-dimensional PHS. For simplicity, dependencies on spatial and temporal variables will frequently be omitted to improve readability.

2.1 Foundations of beam models

In linear elasticity, the displacement field $\mathbf{u}(X,t) = [\mathbf{u}_1 \ \mathbf{u}_2 \ \mathbf{u}_3]^\top \in \mathbb{R}^3$ describes the small displacements of each point $X = \{\zeta_1, \zeta_2, \zeta_3\}$ in a body of volume $\forall \subset \mathbb{R}^3$ relative to a reference configuration. For small strains, the deformation is characterized by the symmetric, infinitesimal strain tensor $\underline{\varepsilon}(X,t) \in \mathbb{R}^{3\times3}$ with components:

$$\varepsilon_{ij} = \frac{1}{2}\left(\frac{\partial \mathbf{u}_i}{\partial \zeta_j} + \frac{\partial \mathbf{u}_j}{\partial \zeta_i}\right), \quad \text{with } i,j = (1,2,3). \tag{1}$$

Assuming Hooke's law under linear isotropic elastic material, the stress-strain relationship is given by $\underline{\sigma}(X,t) = \underline{\underline{C}} : \underline{\varepsilon}(X,t)$, where $\underline{\sigma}(X,t) \in \mathbb{R}^{3\times3}$ is the stress tensor and $\underline{\underline{C}} : \mathbb{R}^{3\times3} \to \mathbb{R}^{3\times3}$ is the fourth-order constitutive tensor, characterized by two independent parameters, Young's modulus E and Poisson's ratio ν. The Voigt-strain vector is defined as $\varepsilon = [\varepsilon_{11} \ \ \varepsilon_{22} \ \ \varepsilon_{33} \ \ 2\varepsilon_{12} \ \ 2\varepsilon_{13} \ \ 2\varepsilon_{23}]^\top$ (Belytschko et al., 2014, Appendix 1). In linear elasticity with constraints, the extended Hamilton's principle provides a systematic way to derive the equations of motion by incorporating constraints into the variational formulation. This principle states that the evolution of the displacement field $\mathbf{u}(X,t)$ between two specific times t_1 and t_2 is a stationary point of an action functional, leading to (Bedford, 1985):

$$\delta \int_{t_1}^{t_2} (T - U + W_E - C_\lambda)\, dt = 0, \tag{2}$$

subject to $\delta\mathbf{u}(X,t_1) = \delta\mathbf{u}(X,t_2) = 0$ for all $X \in \forall$, and $\delta\mathbf{u}(S,t) = 0$ for $S \in \Gamma_D$, with Γ_D the Dirichlet boundary surface of the volume $\forall$. To be more concise, the expressions for the kinetic energy T, the elastic energy U, the external work W_E and the constraint functional C_λ will be introduced later. For a more comprehensive review on these topics, refer to (Bedford, 1985; Reddy, 2013, 2017).

2.2 Infinite-dimensional port-Hamiltonian beam models

The infinite-dimensional PH representations of beam models presented here belong to the class of PHS described in (Ponce et al., 2024).

Definition 1 (Ponce et al., 2024). Let $\mathtt{x} = \{\zeta_1, \ldots, \zeta_\ell\}$ be orthogonal coordinate axes, $\Omega \subset \mathbb{R}^\ell$ an open set, and $v(\mathtt{x}) \in \mathbb{R}^m$ and $w(\mathtt{x}) \in \mathbb{R}^n$ two smooth fields with compact support in Ω. The differential operator $\mathcal{F} : L^2(\Omega) \to L^2(\Omega)$ and its formal adjoint $\mathcal{F}^*$ are given by:

$$\mathcal{F}\, w(\mathtt{x}) = F_0\, w(\mathtt{x}) + \textstyle\sum_{k=1}^{\ell} \sum_{i=1}^{N} F_k(i)\, \partial_k^i\, w(\mathtt{x}), \tag{3}$$

$$\mathcal{F}^* v(\mathtt{x}) = F_0^\top v(\mathtt{x}) + \textstyle\sum_{k=1}^{\ell} \sum_{i=1}^{N} (-1)^i F_k(i)^\top \partial_k^i\, v(\mathtt{x}), \tag{4}$$

with $\partial_k^i = \partial^i / \partial \zeta_k^i$, F_0, $F_k(i) \in \mathbb{R}^{m\times n}$ and N the order of the highest derivative with respect to any ζ_k.

Lemma 1 (Ponce et al., 2024). Let $\Omega \subset \mathbb{R}^\ell$ be an ℓ-dimensional domain, its boundary $\partial\Omega$ and $\bar{\Omega} = \Omega \cup \partial\Omega$ the closure, such that $\mathtt{x} \in \Omega$ and $\mathtt{s} \in \partial\Omega$. Then for any $v(\mathtt{x}) \in \mathbb{R}^m$ and $w(\mathtt{x}) \in \mathbb{R}^n$ defined in $\bar{\Omega}$ we have that:

$$\int_\Omega \left(v^\top \mathcal{F}\, w - w^\top \mathcal{F}^* v\right) d\mathtt{x} = \int_{\partial\Omega} \mathcal{B}(w)^\top \mathcal{Q}_\partial\, \mathcal{B}(v)\, d\mathtt{s}, \tag{5}$$

where $\mathcal{B}(\cdot)$ is a linear differential operator defined as:

$$\mathcal{B}(\cdot) = \left[(\cdot)\ \partial_1(\cdot) \cdots \partial_\ell(\cdot)\ \partial_1^2(\cdot) \cdots \partial_\ell^2(\cdot) \cdots\ \partial_1^{N-1}(\cdot) \cdots \partial_\ell^{N-1}(\cdot)\right]^\top, \tag{6}$$

and $\mathcal{Q}_\partial(\mathtt{s}) \in \mathbb{R}^{n+(N-1)n\ell \times m+(N-1)m\ell}$ is a matrix given by:

$$\mathcal{Q}_\partial(\mathtt{s}) = \begin{bmatrix} F_\partial(\mathtt{s}) & -W_2(\mathtt{s}) & W_3(\mathtt{s}) & \cdots & (-1)^{N-1} W_N(\mathtt{s}) \\ V_2(\mathtt{s}) & -\Lambda_3(\mathtt{s}) & \Lambda_4(\mathtt{s}) & \iddots & 0 \\ \vdots & \vdots & \iddots & & \vdots \\ V_{N-1}(\mathtt{s}) & -\Lambda_N(\mathtt{s}) & 0 & & \vdots \\ V_N(\mathtt{s}) & 0 & 0 & \cdots & 0 \end{bmatrix} \tag{7}$$

with $F_\partial(\mathtt{s}) \in \mathbb{R}^{n\times m}$, $W_i(\mathtt{s}) \in \mathbb{R}^{n\times m\ell}$, $V_i(\mathtt{s}) \in \mathbb{R}^{n\ell\times m}$, and $\Lambda_i(\mathtt{s}) \in \mathbb{R}^{n\ell\times m\ell}$ defined as:

$$F_\partial(\mathtt{s}) = \textstyle\sum_{k=1}^{\ell} F_k(1)^\top \hat{n}_k(\mathtt{s}), \quad W_i(\mathtt{s}) = \left[F_1(i)^\top \hat{n}_1(\mathtt{s}) \ \cdots \ F_\ell(i)^\top \hat{n}_\ell(\mathtt{s})\right]$$

$$V_i(\mathtt{s}) = \begin{bmatrix} F_1(i)^\top \hat{n}_1(\mathtt{s}) \\ \vdots \\ F_\ell(i)^\top \hat{n}_\ell(\mathtt{s}) \end{bmatrix}, \quad \Lambda_i(\mathtt{s}) = \begin{bmatrix} F_1(i)^\top \hat{n}_1(\mathtt{s}) & & 0 \\ & \ddots & \\ 0 & & F_\ell(i)^\top \hat{n}_\ell(\mathtt{s}) \end{bmatrix} \tag{8}$$

where $\hat{n}_k(\mathtt{s})$ is the component of the outward unit normal vector to the boundary projected on the axis ζ_k.

Corollary 1 (Ponce et al., 2024). When the differential operator $\mathcal{F}$ is of first order ($N = 1$), (5) reduces to:

$$\int_\Omega \left(v^\top \mathcal{F}\, w - w^\top \mathcal{F}^* v\right) d\mathtt{x} = \int_{\partial\Omega} w^\top F_\partial\, v\, d\mathtt{s}. \tag{9}$$

Note that (5) and (9) are some of the many manifestations of the integration by parts rule.

Theorem 1 (Ponce et al., 2024). The dynamics of the beams define infinite-dimensional linear PHS of the form:

$$\underbrace{\begin{bmatrix}\dot{p}\\ \dot{\epsilon}\end{bmatrix}}_{\dot{x}} = \underbrace{\begin{bmatrix}0 & -\mathcal{F}^*\\ \mathcal{F} & 0\end{bmatrix}}_{\mathcal{J}=-\mathcal{J}^*} \underbrace{\begin{bmatrix}e_p\\ e_\epsilon\end{bmatrix}}_{\delta_x H(x)} \tag{10}$$

$$H(x) = \frac{1}{2}\int_\Omega \left(p^\top \mathcal{M}^{-1} p + \epsilon^\top \mathcal{K}\epsilon\right) d\mathtt{x}, \tag{11}$$

$$\dot{H} = \int_{\partial\Omega} \mathcal{B}(e_p)^\top \mathcal{Q}_\partial\, \mathcal{B}(e_\epsilon)\, d\mathtt{s} = \int_{\partial\Omega} y_\partial^\top u_\partial\, d\mathtt{s}, \tag{12}$$

where $\mathcal{J} = -\mathcal{J}^*$ is the skew-adjoint linear differential operator (interconnection operator), $\delta_x H(x)$ denotes the variational derivative of $H(x)$ with respect to $x(\mathtt{x},t)$, and $\dot{H}$ is the energy balance with $u_\partial(\mathtt{s},t)$, $y_\partial(\mathtt{s},t) \in \mathbb{R}^n$ the power-conjugated boundary input and output, respectively. The total energy is given by the Hamiltonian $H(x)$, where $\mathcal{M}(\mathtt{x}) = \mathcal{M}(\mathtt{x})^\top > 0 \in \mathbb{R}^{n\times n}$ is the mass density matrix, and $\mathcal{K}(\mathtt{x}) = \mathcal{K}(\mathtt{x})^\top > 0 \in \mathbb{R}^{m\times m}$ is the stiffness density matrix. From energy variables, $p(\mathtt{x},t) = \mathcal{M}(\mathtt{x})\dot{r}(\mathtt{x},t) \in \mathbb{R}^n$ is the generalized momentum with $r(\mathtt{x},t) \in \mathbb{R}^n$ the generalized displacement, and $\epsilon(\mathtt{x},t) = \mathcal{F}\, r(\mathtt{x},t) \in \mathbb{R}^m$ is the generalized strain (kinematics, strain-displacement relation). From co-energy variables, $e_p(\mathtt{x},t) = \mathcal{M}(\mathtt{x})^{-1}\, p(\mathtt{x},t) = \dot{r}(\mathtt{x},t)$ is the generalized velocity, and $e_\epsilon(\mathtt{x},t) = \mathcal{K}(\mathtt{x})\, \epsilon(\mathtt{x},t)$ is the generalized stress (Hooke's law, stress-strain relation).

In the following, we present the key variables of the PHS representations for the Timoshenko, Euler-Bernoulli, and Rayleigh beam models. For further details, please refer to (Ponce et al., 2024) and (Ponce et al., 2023, Appendix D).

Timoshenko beam: The displacement field of the Timoshenko beam is given by:

$$\mathbf{u}(X,t) = \underbrace{\begin{bmatrix}-\zeta_3 & 0\\ 0 & 0\\ 0 & 1\end{bmatrix}}_{\bar{M}_1} \underbrace{\begin{bmatrix}\psi(\mathtt{x},t)\\ w_0(\mathtt{x},t)\end{bmatrix}}_{r(\mathtt{x},t)}, \tag{13}$$

where $\psi(\mathtt{x},t)$ represents the rotation angle of the cross section and $w_0(\mathtt{x},t)$ is the vertical displacement. Using (13) together with (1) lead to the nonzero Voigt-strains:

$$\begin{bmatrix}\varepsilon_{11}(X,t)\\ 2\varepsilon_{13}(X,t)\end{bmatrix} = \underbrace{\begin{bmatrix}-\zeta_3 & 0\\ 0 & 1\end{bmatrix}}_{\bar{M}_2} \underbrace{\begin{bmatrix}\partial_1 & 0\\ -1 & \partial_1\end{bmatrix}}_{\mathcal{F}} \underbrace{\begin{bmatrix}\psi(\mathtt{x},t)\\ w_0(\mathtt{x},t)\end{bmatrix}}_{r(\mathtt{x},t)}, \tag{14}$$

where $\epsilon(\mathtt{x},t) = \mathcal{F}r(\mathtt{x},t) \in \mathbb{R}^2$, being $\epsilon_1(\mathtt{x},t) = \partial_1\psi$ the generalized bending strain, and $\epsilon_2(\mathtt{x},t) = \partial_1 w_0 - \psi$ the generalized shearing strain. The mass and stiffness density matrices are obtained from:

$$\mathcal{M}(\mathtt{x}) = \rho(\mathtt{x}) \int_A \bar{M}_1^\top \bar{M}_1\, dA = \begin{bmatrix}\rho(\mathtt{x})I(\mathtt{x}) & 0\\ 0 & \rho(\mathtt{x})A(\mathtt{x})\end{bmatrix}, \tag{15}$$

$$\mathcal{K}(\mathtt{x}) = \int_A \bar{M}_2^\top \underbrace{\begin{bmatrix}E & 0\\ 0 & \kappa G\end{bmatrix}}_{C} \bar{M}_2\, dA = \begin{bmatrix}EI(\mathtt{x}) & 0\\ 0 & \kappa G A(\mathtt{x})\end{bmatrix}, \tag{16}$$

where $\rho(\mathtt{x})$ is the density of the material, $A(\mathtt{x})$ is the cross section area, $I(\mathtt{x})$ is the second moment of inertia of the cross section, C is the constitutive matrix, $G = \frac{E}{2(1+\nu)}$ is the shear modulus, and κ is a correction factor.

Euler-Bernoulli beam: The displacement field of the Euler-Bernoulli beam is given by:

$$\mathbf{u}(X,t) = \underbrace{\begin{bmatrix}-\zeta_3 & 0\\ 0 & 0\\ 0 & 1\end{bmatrix}}_{\bar{M}_1} \begin{bmatrix}\partial_1 w_0(\mathtt{x},t)\\ w_0(\mathtt{x},t)\end{bmatrix}, \tag{17}$$

where $\partial_1 w_0(\mathtt{x},t)$ represents the rotation angle of the cross section (always normal to the neutral line) and $w_0(\mathtt{x},t)$ is the vertical displacement. Using (13) together with (1) lead to the nonzero Voigt-strain:

$$\varepsilon_{11}(X,t) = -\zeta_3\, \partial_1^2 w_0(\mathtt{x},t), \tag{18}$$

where the generalized displacement is identified as $r(\mathtt{x},t) = w_0(\mathtt{x},t)$. Thus, $\epsilon(\mathtt{x},t) = \mathcal{F}r(\mathtt{x},t) \in \mathbb{R}^1$, with $\mathcal{F} = \partial_1^2$ and $\epsilon(\mathtt{x},t) = \partial_1^2 w_0$, the latter representing the generalized bending strain. The mass density matrix for the Euler-Bernoulli beam is derived from (15) by disregarding the rotary inertia term $\rho(\mathtt{x})I(\mathtt{x})$, and the stiffness density matrix accounts solely for the bending strain. Thus:

$$\mathcal{M}(\mathtt{x}) = \rho(\mathtt{x})A(\mathtt{x}), \quad \mathcal{K}(\mathtt{x}) = EI(\mathtt{x}). \tag{19}$$

Remark 1 The Euler-Bernoulli beam model is a simplified (degenerate) model because it neglects rotary inertia. In contrast, the Rayleigh beam includes it, providing a more accurate, and energy-consistent representation.

Rayleigh beam: The displacement field $\mathbf{u}(X,t)$, the nonzero strain $\varepsilon_{11}(X,t)$, and the mass density matrix $\mathcal{M}(\mathtt{x})$ of the Rayleigh beam are the same as defined in (17), (18), and (15), respectively. The nonzero strain can be written equivalently as:

$$\varepsilon_{11}(X,t) = \underbrace{-\frac{\zeta_3}{2}}_{\bar{M}_2} \underbrace{\begin{bmatrix}\partial_1 & \partial_1^2\end{bmatrix}}_{\mathcal{F}} \underbrace{\begin{bmatrix}\partial_1 w_0(\mathtt{x},t)\\ w_0(\mathtt{x},t)\end{bmatrix}}_{r(\mathtt{x},t)}, \tag{20}$$

which leads to the generalized strain $\epsilon(\mathtt{x},t) = \mathcal{F}r(\mathtt{x},t) = 2\,\partial_1^2 w_0(\mathtt{x},t)$. The stiffness density matrix is obtained from:

$$\mathcal{K}(\mathtt{x}) = \int_A \bar{M}_2^\top E \bar{M}_2\, dA = \frac{EI(\mathtt{x})}{4}. \tag{21}$$

Notice that $\mathcal{F}$ is a $m \times n = 1 \times 2$ second-order differential operator. This results in the previously discussed challenges, including difficulties in ensuring numerical stability and physical validity when applying mixed FEM.

3. MODELING AND DISCRETIZATION OF THE RAYLEIGH BEAM

First, we derive the infinite-dimensional PH-DAE model for the Rayleigh beam using the Timoshenko beam model as starting point. Next, we propose a structure-preserving discretization using a mixed FEM approach, allowing for the discretization of both the dynamic equations and the algebraic constraint.

3.1 Infinite-dimensional Rayleigh beam model as PH-DAE

First of all, assume that $\partial\Omega = \partial\Omega_D \cup \partial\Omega_N$ and $\partial\Omega_D \cap \partial\Omega_N = \{\emptyset\}$ with $\{\emptyset\}$ the empty set, where $\partial\Omega_D$ and $\partial\Omega_N$ are the boundary portions where Dirichlet and Neumann BC are imposed, respectively. For the Timoshenko beam model, the generalized displacement field is defined as

$r = [\psi \;\; w_0]^\top$, with kinetic energy T, elastic energy U, and external work W_E expressed as follows:

$$T = \frac{1}{2}\int_\Omega \dot{r}^\top \mathcal{M}\dot{r}\, d\mathtt{x},\; U = \frac{1}{2}\int_\Omega \epsilon^\top \mathcal{K}\,\epsilon\, d\mathtt{x},\; W_E = \int_{\partial\Omega_N} \tau_N^\top\, r\, d\mathtt{s},$$

where $\tau_N(\mathtt{s},t) \in \mathbb{R}^n$ is the generalized boundary traction imposed on $\partial\Omega_N$, representing the Neumann BC. According with the Rayleigh beam's kinematic assumptions, the constraint imposed is:

$$\gamma(r) = \partial_1 w_0 - \psi = \mathcal{L}\, r = 0, \tag{22}$$

where $\mathcal{L} = [-1 \quad \partial_1]$ is a first-order differential operator of the same class as defined in Definition 1. This constraint is equivalent to set the generalized shearing strain $\epsilon_2 = \partial_1 w_0 - \psi = 0$. With the above, the constraint functional is written as: $C_\lambda = \int_\Omega \gamma \cdot \lambda\, d\Omega$, where $\lambda(\mathtt{x},t) \in \mathbb{R}$ is the Lagrange multiplier introduced to impose the constraint $\gamma(r) = 0$ on Ω. In the next proposition, we state the infinite-dimensional PH-DAE representation of the Rayleigh beam.

Proposition 1 Let $x = [p^\top \;\; \epsilon^\top \;\; \lambda]^\top \in \mathbb{R}^{n+m+1}$ be the energy variables, and $\mathcal{Z}(x) = [e_p^\top \; e_\epsilon^\top \; \lambda]^\top \in \mathbb{R}^{n+m+1}$ be the effort function. The system's dynamics define an infinite-dimensional linear PH-DAE of the form:

$$\underbrace{\begin{bmatrix} I_n & 0 & 0 \\ 0 & I_m & 0 \\ 0 & 0 & 0 \end{bmatrix}}_{\mathcal{E}} \underbrace{\begin{bmatrix} \dot{p} \\ \dot{\epsilon} \\ \dot{\lambda} \end{bmatrix}}_{\dot{x}} = \underbrace{\begin{bmatrix} 0 & -\mathcal{F}^* & -\mathcal{L}^* \\ \mathcal{F} & 0 & 0 \\ \mathcal{L} & 0 & 0 \end{bmatrix}}_{\mathcal{J}=-\mathcal{J}^*} \underbrace{\begin{bmatrix} e_p \\ e_\epsilon \\ \lambda \end{bmatrix}}_{\mathcal{Z}(x)} \tag{23}$$

$$u_\partial = [\tau_N^\top \;\; v_D^\top]^\top, \quad y_\partial = [v_N^\top \;\; \tau_D^\top]^\top, \tag{24}$$

$$H(x) = \frac{1}{2}\int_\Omega \left(p^\top \mathcal{M}^{-1} p + \epsilon^\top \mathcal{K}\epsilon\right) d\mathtt{x}, \tag{25}$$

where $I_n \in \mathbb{R}^{n\times n}$, $I_m \in \mathbb{R}^{m\times m}$ are identity matrices, and:

$$\mathcal{L} = [-1 \;\; \partial_1],\; \mathcal{F} = \begin{bmatrix} \partial_1 & 0 \\ -1 & \partial_1 \end{bmatrix},\; \mathcal{M} = \begin{bmatrix} \rho I & 0 \\ 0 & \rho A \end{bmatrix},\; \mathcal{K} = \begin{bmatrix} EI & 0 \\ 0 & \kappa GA \end{bmatrix}.$$

$\tau_D(\mathtt{s},t)$, $\tau_N(\mathtt{s},t)$ and $v_D(\mathtt{s},t)$, $v_N(\mathtt{s},t) \in \mathbb{R}^n$ are the generalized boundary tractions and velocities, defined as:

$$\begin{aligned} \tau_N &= F_\partial\, e_\epsilon + L_\partial \lambda, \quad v_N = e_p \;\text{ (both on } \partial\Omega_N), \\ \tau_D &= F_\partial\, e_\epsilon + L_\partial \lambda, \quad v_D = e_p \;\text{ (both on } \partial\Omega_D), \end{aligned} \tag{26}$$

with $L_\partial = [0 \;\; \hat{n}_1]^\top$ as the boundary matrix associated with $\mathcal{L}$ according to Lemma 1.

Proof. The proof consists in applying the extended Hamilton's principle in (2). From the expression for kinetic energy we have: $\delta\int_{t_1}^{t_2} T\, dt = \int_{t_1}^{t_2}\int_\Omega \delta\dot{r}^\top \mathcal{M}\dot{r} d\mathtt{x}\, dt$, where integrating by parts w.r.t. time we obtain: $\delta\int_{t_1}^{t_2} T\, dt = -\int_{t_1}^{t_2}\int_\Omega \delta r^\top \mathcal{M}\ddot{r} d\mathtt{x}\, dt - \int_\Omega \delta r^\top \mathcal{M}\dot{r} d\mathtt{x}|_{t_1}^{t_2}$, where the last term vanishes due to $\delta r(\mathtt{x},t_1) = \delta r(\mathtt{x},t_2) = 0$ for all $\mathtt{x} \in \Omega$. From the expression for elastic energy U we have: $\delta U = \int_\Omega e_\epsilon^\top \mathcal{F}\delta r\, d\mathtt{x}$, where applying Lemma 1 we obtain: $\delta U = \int_\Omega \delta r^\top \mathcal{F}^* e_\epsilon\, d\mathtt{x} + \int_{\partial\Omega_N} \delta r^\top F_\partial\, e_\epsilon\, d\mathtt{s}$. From the expression for the external virtual work we obtain: $\delta W_E = \int_{\partial\Omega_N} \delta r^\top \tau_N\, d\mathtt{s}$. From the expression for the constraint functional we have: $\delta C_\lambda = \int_\Omega \delta\lambda^\top \mathcal{L}\, r\, d\mathtt{x} + \int_\Omega \lambda^\top \mathcal{L}\,\delta r\, d\mathtt{x}$, where applying Lemma 1 to the second term we obtain: $\delta C_\lambda = \int_\Omega \delta\lambda^\top \mathcal{L}\, r\, d\mathtt{x} + \int_\Omega \delta r^\top \mathcal{L}^*\lambda\, d\mathtt{x} + \int_{\partial\Omega_N} \delta r^\top L_\partial \lambda\, d\mathtt{s}$. Applying the extended Hamilton's principle we obtain:

$$\int_{t_1}^{t_2}\left[\int_\Omega \left[\delta r^\top(-\mathcal{M}\ddot{r} - \mathcal{F}^* e_\epsilon - \mathcal{L}^*\lambda) - \delta\lambda^\top \mathcal{L}\, r\right] d\mathtt{x} \;\; ... \right.$$
$$\left. ... \; - \int_{\partial\Omega_N} \delta r^\top (F_\partial\, e_\epsilon + L_\partial\lambda - \tau_N)\, d\mathtt{s}\right] dt = 0.$$

Recalling that $p = \mathcal{M}\dot{r}, \epsilon = \mathcal{F}r, \dot{r} = e_p,\; \dot{\gamma} = \mathcal{L}\dot{r} = 0$, and applying the fundamental lemma of variational calculus to the previous expression, it leads to the infinite-dimensional PH-DAE stated in (23). Since $\delta_x H(x) = \mathcal{E}^\top \mathcal{Z}(x) = [e_p^\top \;\; e_\epsilon^\top \;\; 0]^\top$, from the energy balance we get: $\dot{H} = \int_\Omega \dot{x}^\top \delta_x H\, d\Omega = \int_{\partial\Omega} y_\partial^\top u_\partial\, d\mathtt{s}$, with u_∂ and y_∂ defined in (24) and (26). ■

Observe that the kinetic energy can be separated into $T = T_r + T_t$, the rotational and translational parts, respectively:

$$T_r = \frac{1}{2}\int_\Omega \frac{p_1^2}{\rho I}\, d\mathtt{x} = \frac{1}{2}\int_\Omega \rho I \dot{\psi}^2\, d\mathtt{x} = \frac{1}{2}\int_\Omega \rho I(\partial_1 \dot{w}_0)^2\, d\mathtt{x},$$
$$T_t = \frac{1}{2}\int_\Omega \frac{p_2^2}{\rho A}\, d\mathtt{x} = \frac{1}{2}\int_\Omega \rho A\, \dot{w}_0{}^2\, d\mathtt{x},$$

and the elastic energy into $U = U_b + U_s$, the bending and shearing parts, respectively:

$$U_b = \frac{1}{2}\int_\Omega EI\epsilon_1^2\, d\mathtt{x} = \frac{1}{2}\int_\Omega EI(\partial_1\psi)^2\, d\mathtt{x} = \frac{1}{2}\int_\Omega EI(\partial_1^2 w_0)^2 d\mathtt{x},$$
$$U_s = \frac{1}{2}\int_\Omega \kappa GA\,\epsilon_2^2\, d\mathtt{x} = \frac{1}{2}\int_\Omega \kappa GA\,(\partial_1 w_0 - \psi)^2\, d\mathtt{x} = 0,$$

which is energetically consistent with the Rayleigh beam.

3.2 Finite-dimensional Rayleigh beam model as PH-DAE

The structure-preserving mixed FEM scheme proposed here builds on the work of (Thoma and Kotyczka, 2022), which addresses the structure-preserving spatial discretization of linear PHS with first-order differential operators. This approach incorporates mixed boundary conditions and uses $\epsilon(\mathtt{x},t) = \mathcal{C}_\epsilon(\mathtt{x}) e_\epsilon(\mathtt{x},t)$, where $\mathcal{C}_\epsilon(\mathtt{x}) = \mathcal{K}(\mathtt{x})^{-1}$ is the compliance density matrix. Before presenting the weak form of (23) and its finite-dimensional approximation, key concepts from FEM are reviewed.

3.2.1. Finite element method

Consider a mesh with n_e elements, NN^e number of nodes per element $\Omega^e \subset \Omega$, and the local approximations:

$$e_p^e = N_p^e(\mathtt{x})\,\hat{e}_p^e(t), \quad e_\epsilon^e = N_e^e(\mathtt{x})\,\hat{e}_\epsilon^e(t), \quad \lambda^e = N_\lambda^e(\mathtt{x})\,\hat{\lambda}^e(t),$$
$$\tau_N^e = N_{\tau_N}^e(\mathtt{s})\,\hat{\tau}_N^e(t),\; v_D^e = N_{v_D}^e(\mathtt{s})\,\hat{v}_D^e(t),$$

where $N_p^e(\mathtt{x})$, $N_{\tau_N}^e(\mathtt{s})$, $N_{v_D}^e(\mathtt{s}) \in \mathbb{R}^{n\times nNN^e}$, $N_e^e(\mathtt{x}) \in \mathbb{R}^{m\times mNN^e}$, and $N_\lambda^e(\mathtt{x}) \in \mathbb{R}^{1\times NN^e}$ are the local shape functions; $\hat{e}_p^e(t) \in \mathbb{R}^{nNN^e}$ and $\hat{e}_\epsilon^e \in \mathbb{R}^{mNN^e}$ are the local co-energy variables on Ω^e, $\hat{\lambda}^e \in \mathbb{R}^{NN^e}$ is the local Lagrange multiplier on Ω^e, and $\hat{\tau}_N^e(t)$ and $\hat{v}_D^e(t) \in \mathbb{R}^{nNN^e}$ are the local BC on $\partial\Omega_N^e$ and $\partial\Omega_D^e$, respectively. Denoting NN_Ω, $NN_{\partial\Omega_N}$ and $NN_{\partial\Omega_D}$ as the total number of nodes on Ω, $\partial\Omega_N$ and $\partial\Omega_D$, respectively; $N_\Omega = nNN_\Omega$, $M_\Omega = mNN_\Omega$, $N_{\partial\Omega_N} = nNN_{\partial\Omega_N}$ and $N_{\partial\Omega_D} = nNN_{\partial\Omega_D}$ define the dimension of the approximated variables on Ω, $\partial\Omega_N$ and $\partial\Omega_D$. Lastly, consider the relations:

$$\hat{e}_p^e(t) = L_p^e\,\hat{e}_p(t), \quad \hat{e}_\epsilon^e(t) = L_e^e\,\hat{e}_\epsilon(t), \quad \hat{\lambda}^e(t) = L_\lambda^e\,\hat{\lambda}(t),$$
$$\hat{\tau}_N^e(t) = L_{\tau_N}^e\,\hat{\tau}_N(t),\; \hat{v}_D^e(t) = L_{v_D}^e\,\hat{v}_D(t),$$

where $\hat{e}_p(t) \in \mathbb{R}^{N_\Omega}$, $\hat{e}_\epsilon(t) \in \mathbb{R}^{M_\Omega}$, $\hat{\lambda}(t) \in \mathbb{R}^{NN_\Omega}$, $\hat{\tau}_N(t) \in \mathbb{R}^{N_{\partial\Omega_N}}$ and $\hat{v}_D(t) \in \mathbb{R}^{N_{\partial\Omega_D}}$ are the global vectors; and $L_p^e \in \mathbb{R}^{nNN^e \times N_\Omega}$, $L_e^e \in \mathbb{R}^{mNN^e \times M_\Omega}$, $L_\lambda^e \in \mathbb{R}^{NN^e \times NN_\Omega}$, $L_{\tau_N}^e \in \mathbb{R}^{nNN^e \times N_{\partial\Omega_N}}$ and $L_{v_D}^e \in \mathbb{R}^{nNN^e \times N_{\partial\Omega_D}}$ are the location (assembly) matrices of FEM.

3.2.2. Structure-preserving mixed FEM

The local weak form of (23) (defined in each element) is given by:

$$\delta P_p^e(e_p^e, e_\epsilon^e, \lambda^e) = \int_{\Omega^e} \delta e_p^e \cdot (\dot{p}^e + \mathcal{F}^* e_\epsilon^e + \mathcal{L}^* \lambda^e)\, d\mathbf{x} \,... + \int_{\partial\Omega_N^e} \delta e_p^e \cdot (F_\partial\, e_\epsilon^e + L_\partial \lambda^e - \tau_N^e)\, d\mathbf{s}, \quad (27)$$

$$\delta P_e^e(e_p^e, e_\epsilon^e, \lambda^e) = \int_{\Omega^e} \delta e_\epsilon^e \cdot (\dot{\epsilon}^e - \mathcal{F}\, e_p^e)\, d\mathbf{x} \,... + \int_{\partial\Omega_D^e} \delta e_\epsilon^e \cdot F_\partial^\top (e_p^e - v_D^e)\, d\mathbf{s}, \quad (28)$$

$$\delta P_\lambda^e(e_p^e, e_\epsilon^e, \lambda^e) = -\int_{\Omega^e} \delta\lambda^e \cdot \mathcal{L}\, e_p^e\, d\mathbf{x} \,... + \int_{\partial\Omega_D^e} \delta\lambda^e \cdot L_\partial^\top (e_p^e - v_D^e)\, d\mathbf{s}, \quad (29)$$

where each term δP_p^e, δP_e^e, and δP_λ^e represent the local virtual power due to independent variations of e_p^e, e_ϵ^e and λ^e, respectively.

Proposition 2 The mixed FEM discretization of (23) based on the weak formulation (27)-(29), using the local approximations presented in Section 3.2.1, leads to the finite-dimensional PH-DAE of the form:

$$[\hat{E}] \underbrace{\begin{bmatrix} \dot{\hat{p}} \\ \dot{\hat{\epsilon}} \\ \dot{\hat{\lambda}} \end{bmatrix}}_{\dot{\hat{x}}} = \underbrace{\begin{bmatrix} 0 & -\hat{F}^\top & -\hat{L}^\top \\ \hat{F} & 0 & 0 \\ \hat{L} & 0 & 0 \end{bmatrix}}_{\hat{J}=-\hat{J}^\top} \underbrace{\begin{bmatrix} \hat{e}_p \\ \hat{e}_\epsilon \\ \hat{\lambda} \end{bmatrix}}_{\hat{Z}(\hat{x})} + \underbrace{\begin{bmatrix} \hat{B}_N & 0 \\ 0 & \hat{B}_D \\ 0 & \hat{B}_\lambda \end{bmatrix}}_{\hat{G}} \underbrace{\begin{bmatrix} \hat{\tau}_N \\ \hat{v}_D \end{bmatrix}}_{\hat{u}_\partial} \quad (30)$$

$$\hat{y}_\partial = \hat{G}^\top \hat{Z}(\hat{x}) = \begin{bmatrix} \hat{B}_N^\top \hat{e}_p + \hat{B}_\lambda^\top \hat{\lambda} \\ \hat{B}_D^\top \hat{e}_\epsilon \end{bmatrix} = \begin{bmatrix} \hat{v}_N \\ \hat{\tau}_D \end{bmatrix},$$

$$\hat{H}(\hat{x}) = \frac{1}{2}\, \hat{p}^\top \hat{M}^{-1} \hat{p} + \frac{1}{2}\, \hat{\epsilon}^\top \hat{C}_\epsilon^{-1} \hat{\epsilon}, \quad (31)$$

where $\hat{p}(t) = \hat{M}\hat{e}_p(t)$ and $\hat{\epsilon}(t) = \hat{C}_\epsilon\, \hat{e}_\epsilon(t)$ are the discrete generalized momentum and strain variables, respectively. The involved matrices are defined as:

$$\hat{E} = \mathrm{diag}\,(I_{N_\Omega},\, I_{M_\Omega},\, 0_{NN_\Omega}), \quad (32)$$

$$\hat{M} = \sum_{e=1}^{n_e} (L_p^e)^\top \int_{\Omega^e} N_p^e(\mathbf{x})^\top \mathcal{M}(\mathbf{x}) N_p^e(\mathbf{x})\, d\mathbf{x}\, L_p^e, \quad (33)$$

$$\hat{C}_\epsilon = \sum_{e=1}^{n_e} (L_e^e)^\top \int_{\Omega^e} N_e^e(\mathbf{x})^\top \mathcal{C}_\epsilon(\mathbf{x}) N_e^e(\mathbf{x})\, d\mathbf{x}\, L_e^e, \quad (34)$$

$$\hat{B}_N = \sum_{e=1}^{n_e} (L_p^e)^\top \int_{\partial\Omega_N^e} N_p^e(\mathbf{s})^\top N_{\tau_N}^e(\mathbf{s})\, d\mathbf{s}\, L_{\tau_N}^e, \quad (35)$$

$$\hat{B}_D = \sum_{e=1}^{n_e} (L_e^e)^\top \int_{\partial\Omega_D^e} N_e^e(\mathbf{s})^\top F_\partial(\mathbf{s})^\top N_{v_D}^e(\mathbf{s})\, d\mathbf{s}\, L_{v_D}^e, \quad (36)$$

$$\hat{B}_\lambda = \sum_{e=1}^{n_e} (L_\lambda^e)^\top \int_{\partial\Omega_D^e} N_\lambda^e(\mathbf{s})^\top L_\partial(\mathbf{s})^\top N_{v_D}^e(\mathbf{s})\, d\mathbf{s}\, L_{v_D}^e, \quad (37)$$

$$\hat{F}^\top = \sum_{e=1}^{n_e} (L_p^e)^\top \left(\int_{\Omega^e} (\mathcal{F} N_p^e(\mathbf{x}))^\top N_e^e(\mathbf{x})\, d\mathbf{x} \,... - \int_{\partial\Omega_D^e} N_p^e(\mathbf{s})^\top F_\partial(\mathbf{s}) N_e^e(\mathbf{s})\, d\mathbf{s} \right) L_e^e, \quad (38)$$

$$\hat{L}^\top = \sum_{e=1}^{n_e} (L_p^e)^\top \left(\int_{\Omega^e} (\mathcal{L} N_p^e(\mathbf{x}))^\top N_\lambda^e(\mathbf{x})\, d\mathbf{x} \,... - \int_{\partial\Omega_D^e} N_p^e(\mathbf{s})^\top L_\partial(\mathbf{s}) N_\lambda^e(\mathbf{s})\, d\mathbf{s} \right) L_\lambda^e, \quad (39)$$

where $I_{N_\Omega} \in \mathbb{R}^{N_\Omega \times N_\Omega}$ and $I_{M_\Omega} \in \mathbb{R}^{M_\Omega \times M_\Omega}$ are identity matrices and $0_{NN_\Omega} \in \mathbb{R}^{NN_\Omega \times NN_\Omega}$ is a zero matrix.

Proof. Using Lemma 1 we obtain:

$$\int_{\Omega^e} (\delta e_p^e)^\top \mathcal{F}^* e_\epsilon^e\, d\mathbf{x} = \int_{\Omega^e} (\mathcal{F}\delta e_p^e)^\top e_\epsilon\, d\mathbf{x} - \int_{\partial\Omega_N^e} (\delta e_p^e)^\top F_\partial e_\epsilon\, d\mathbf{s} ... - \int_{\partial\Omega_D^e} (\delta e_p^e)^\top F_\partial e_\epsilon\, d\mathbf{s},$$

$$\int_{\Omega^e} (\delta e_p^e)^\top \mathcal{L}^* \lambda^e\, d\mathbf{x} = \int_{\Omega^e} (\mathcal{L}\delta e_p^e)^\top \lambda\, d\mathbf{x} - \int_{\partial\Omega_N^e} (\delta e_p^e)^\top L_\partial \lambda\, d\mathbf{s} ... - \int_{\partial\Omega_D^e} (\delta e_p^e)^\top L_\partial \lambda\, d\mathbf{s}.$$

Then, replacing the above expressions into (27) and using $\mathcal{F}\,\delta e_p^e(\mathbf{x}, t) = (\mathcal{F} N_p^e(\mathbf{x}))\delta\hat{e}_p^e(t)$, $\hat{e}_p^e(t) = L_p^e \hat{e}_p(t)$ with $\hat{e}_p(t)$ the global vector (analogously the same for the other variables), the global form of (27) becomes $\delta P_p = \sum_{e=1}^{n_e} \delta P_p^e(e_p^e, e_\epsilon^e, \lambda^e) = 0$ and is given by:

$$\delta P_p = \delta\hat{e}_p^\top [\hat{M}\dot{\hat{e}}_p + \hat{F}^\top \hat{e}_\epsilon - \hat{L}^\top \hat{\lambda} - \hat{B}_N \hat{\tau}_N] = 0. \quad (40)$$

Similarly, $\delta P_e = \sum_{e=1}^{n_e} \delta P_e^e(e_p^e, e_\epsilon^e, \lambda^e) = 0$ and $\delta P_\lambda = \sum_{e=1}^{n_e} \delta P_\lambda^e(e_p^e, e_\epsilon^e, \lambda^e) = 0$ are given by:

$$\delta P_e = \delta\hat{e}_\epsilon^\top [\hat{C}_\epsilon \dot{\hat{e}}_\epsilon - \hat{F}\hat{e}_p - \hat{B}_D \hat{v}_D] = 0, \quad (41)$$

$$\delta P_\lambda = -\delta\hat{\lambda}^\top [\hat{L}\dot{\hat{e}}_p + \hat{B}_\lambda \hat{v}_D] = 0. \quad (42)$$

The Hamiltonian in each element is expressed as:

$$H^e(e_p^e, e_\epsilon^e) = \frac{1}{2} \int_{\Omega^e} \left[(e_p^e)^\top \mathcal{M} e_p^e + (e_\epsilon^e)^\top \mathcal{C}_\epsilon e_\epsilon^e \right] d\mathbf{x},$$

then, the total energy of the system is $H = \sum_{e=1}^{n_e} H^e$, and the discrete Hamiltonian is given by:

$$\hat{H}(\hat{e}_p, \hat{e}_\epsilon) = \frac{1}{2}\hat{e}_p^\top \hat{M} \hat{e}_p + \frac{1}{2}\hat{e}_\epsilon^\top \hat{C}_\epsilon \hat{e}_\epsilon. \quad (43)$$

Finally, with the definitions of the discrete generalized momentum and strain variables, equations (40)-(42) define the finite-dimensional PH-DAE in (30), while equation (43) defines the Hamiltonian function in (31). ■

4. SIMULATIONS

For time integration, we use the implicit midpoint rule. For a finite-dimensional DAE system in the form: $S\dot{z} = f(z, t)$, where S is a square singular matrix, we have:

$$S z_{k+1} = S z_k + h f\left(z_m, t_m\right),$$

where $z_m = \frac{1}{2}(z_k + z_{k+1})$ and $t_m = t_0 + kh + \frac{h}{2}$ represent the midpoint values, with t_0 as the initial time, h as the time step, and $k \in \mathbb{N}_+$ an integer. Applying this rule to the PH-DAE in (30) gives:

$$0 = \left(\hat{E} + \frac{h}{2}\hat{J}\hat{Q}\right)\hat{x}_k - \left(\hat{E} - \frac{h}{2}\hat{J}\hat{Q}\right)\hat{x}_{k+1} + h\hat{G}\hat{u}_\partial(t_m), \quad (44)$$

where $\hat{Q} = \text{diag}(\hat{M}^{-1}, \hat{C}_\epsilon^{-1}, I_{NN_\Omega})$ with $I_{NN_\Omega} \in \mathbb{R}^{NN_\Omega \times NN_\Omega}$ an identity matrix. We solve (44) for $\hat{x}_{k+1}$ for all k.

Simulations are conducted with the following parameters: $\rho = 7800\,[kg/m^3]$, $E = 210\,[GPa]$, $\nu = 0.3\,[-]$, $L = 50\,[cm]$, $A = 30\,[mm^2]$, $I = 2.5\,[mm^4]$, $\kappa = 5/6\,[-]$. The beam's BCs are: fixed at $\zeta_1 = 0$, (i.e., $v_D = 0$), and a vertical force applied at $\zeta_1 = L$, given by:

$$\hat{\tau}_N = \begin{bmatrix} 0 \\ 1\sin(5\pi t) \end{bmatrix}, \quad \text{for: } 0 \leq t \leq 0.5\ [s].$$

The discretization uses $n_e = 10$ finite elements with first-order Lagrange polynomials as shape functions, and a time step of $h = 0.01[s]$. Results are shown in Fig. 1.

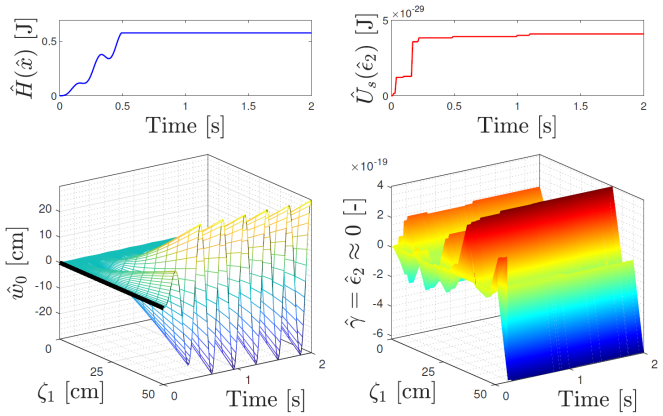

Fig. 1. Simulation results: Rayleigh beam

As shown in Fig. 1, the constraint $\gamma = 0$ is effectively satisfied throughout the spatial domain $\zeta_1 \in \Omega$ and for all time instances, ensuring that the elastic energy contribution due to shear strain, U_s, is negligible. Additionally, the total energy is conserved, and the evolution of the vertical displacement $\hat{w}_0$ results in a consistent deformed configuration for the beam.

5. CONCLUSIONS

This paper has introduced a novel infinite-dimensional PH-DAE model for the Rayleigh beam, along with a structure-preserving mixed FEM discretization approach. By building on the Timoshenko beam model and Hellinger-Reissner-based methods, the proposed framework enables the development of models suitable for both simulation and control design across continuous and discrete domains. The presented simulations demonstrate physically consistent dynamics while satisfying the algebraic constraint. Future directions include investigation of well-posedness, extending this methodology to the Kirchhoff-Rayleigh plate, and leveraging these models in reduced-order energy-based control design, using, for instance, the approaches for PH-DAEs presented in (Wu et al., 2014; Macchelli, 2014; Mehrmann and Unger, 2023).

REFERENCES

Bedford, A. (1985). *Hamilton's principle in continuum mechanics*, volume 139. Springer.

Belytschko, T., Liu, W., Moran, B., and Elkhodary, K. (2014). *Nonlinear finite elements for continua and structures*. John wiley & sons.

Cardoso-Ribeiro, F., Matignon, D., and Pommier-Budinger, V. (2016). Piezoelectric beam with distributed control ports: a power-preserving discretization using weak formulation. *IFAC-PapersOnLine*, 49(8), 290–297.

Christie, I., Griffiths, D., Mitchell, A., and Zienkiewicz, O. (1976). Finite element methods for second order differential equations with significant first derivatives. *International Journal for Numerical Methods in Engineering*, 10(6), 1389–1396.

Duindam, V., Macchelli, A., Stramigioli, S., and Bruyninckx, H. (2009). *Modeling and control of complex physical systems: the port-Hamiltonian approach*. Springer Science & Business Media.

Engel, G., Garikipati, K., Hughes, T., Larson, M., Mazzei, L., and Taylor, R. (2002). Continuous/discontinuous finite element approximations of fourth-order elliptic problems in structural and continuum mechanics with applications to thin beams and plates, and strain gradient elasticity. *Computer Methods in Applied Mechanics and Engineering*, 191(34), 3669–3750.

Golo, G., Talasila, V., van der Schaft, A., and Maschke, B. (2004). Hamiltonian discretization of boundary control systems. *Automatica*, 40(5), 757–771.

Kinon, P., Thoma, T., Betsch, P., and Kotyczka, P. (2024). Generalized Maxwell viscoelasticity for geometrically exact strings: Nonlinear port-Hamiltonian formulation and structure-preserving discretization. *IFAC-PapersOnLine*, 58(6), 101–106.

Labuschagne, A., van Rensburg, N., and van der Merwe, A. (2009). Comparison of linear beam theories. *Mathematical and Computer Modelling*, 49(1-2), 20–30.

Macchelli, A. (2014). Passivity-based control of implicit port-Hamiltonian systems. *SIAM Journal on Control and Optimization*, 52(4), 2422–2448.

Macchelli, A. and Melchiorri, C. (2004). Modeling and control of the Timoshenko beam. The distributed port Hamiltonian approach. *SIAM journal on control and optimization*, 43(2), 743–767.

Mehrmann, V. and Unger, B. (2023). Control of port-Hamiltonian differential-algebraic systems and applications. *Acta Numerica*, 32, 395–515.

Nguyen, A. (2017). *Comparative spectral analysis of flexible structure models: the Euler-Bernoulli beam model, the Rayleigh beam model, and the Timoshenko beam model*. Master's thesis, University of New Hampshire.

Ponce, C., Wu, Y., Le Gorrec, Y., and Ramirez, H. (2023). Port-Hamiltonian modeling of multidimensional flexible mechanical structures defined by linear elastic relations. *arXiv preprint arXiv:2311.03796*.

Ponce, C., Wu, Y., Le Gorrec, Y., and Ramirez, H. (2024). A systematic methodology for port-Hamiltonian modeling of multidimensional flexible linear mechanical systems. *Applied Mathematical Modelling*.

Reddy, J.N. (2013). *An introduction to continuum mechanics*. Cambridge university press.

Reddy, J.N. (2017). *Energy principles and variational methods in applied mechanics*. John Wiley & Sons.

Suri, M. (1990). On the stability and convergence of higher-order mixed finite element methods for second-order elliptic problems. *Mathematics of computation*, 54(189), 1–19.

Thoma, T. and Kotyczka, P. (2022). Explicit port-Hamiltonian FEM-models for linear mechanical systems with non-uniform boundary conditions. *IFAC-PapersOnLine*, 55(20), 499–504.

van der Schaft, A. (2000). Implicit port-controlled Hamiltonian systems. *Journal of the Society of Instrument and Control Engineers*, 39(6), 410–418.

Warsewa, A., Böhm, M., Sawodny, O., and Tarín, C. (2021). A port-Hamiltonian approach to modeling the structural dynamics of complex systems. *Applied Mathematical Modelling*.

Wu, Y., Hamroun, B., Le Gorrec, Y., and Maschke, B. (2014). Port-Hamiltonian system in descriptor form for balanced reduction: Application to a nanotweezer. *IFAC Proceedings Volumes*, 47(3), 11404–11409.

Zienkiewicz, O., Taylor, R., and Zhu, J. (2005). *The finite element method: its basis and fundamentals. Sixth edition*. Elsevier.